

Dynamics of an Inclusion Complex of Chloroform and Cryptophane-E: Evidence for a Strongly Anisotropic van der Waals Bond

Jan Lang,^{†,§} James J. Dechter,[‡] Maria Effemey,[†] and Jozef Kowalewski^{*,†}

Contribution from the Division of Physical Chemistry, Stockholm University, S-106 91 Stockholm, Sweden, and Department of Chemistry, University of Central Oklahoma, Edmond, Oklahoma 73034

Received December 27, 2000. Revised Manuscript Received May 9, 2001

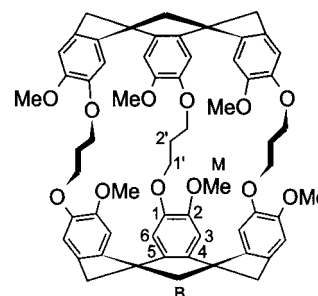
Abstract: The motional dynamics of a van der Waals inclusion complex of cryptophane-E and chloroform has been investigated by a combined NMR exchange and relaxation study. The kinetics of exchange of chloroform between the bulk solution and the complex was investigated by means of proton EXSY measurements. The carbon-13 relaxation of the cryptophane-E host and of the bound chloroform guest was analyzed using the Lipari–Szabo “model-free” approach. For interpretation of the carbon-13 relaxation measurements for chloroform, the chemical-exchange process of complex formation and dissociation had to be taken into account in terms of the modified Bloch equations. It was found that the complex behaves as a single molecule without any significant guest chloroform motion inside the host’s cavity.

Introduction

Understanding different noncovalent bonding interactions has been a challenge for chemists and physicists during the past few decades. Various structures based on this type of bonding to form stable complexes have been designed and investigated. A lot of interest has been centered around hydrogen bonding in water-soluble, biologically relevant systems. Besides that, numerous neutral organic systems have been designed to make use of van der Waals interaction. Such systems, based on calixarene,¹ cyclophane,² crown-ether,³ or even cyclodextrin⁴ matrixes, have already found many interesting applications in molecular recognition and analysis⁵ (sensors, selective electrodes), catalysis,^{6,7} supramolecular chemistry,⁸ and many other fields. Indeed, in most of such systems, various types of noncovalent interactions take place side by side, and it is often difficult to dissect the individual contributions.

Cryptophanes were found to interact strongly with small neutral species in a hydrophobic environment.^{9–16} Globularly

Chart 1. Cryptophane-E^a



^a Carbon atom numbering used for the NMR spectra assignment is shown for the aromatic ring (1–6), propylene linker (1',2'), methylene bridge (B), and methoxy residue (M).

shaped cryptophane molecules consist of two cyclotriveratrylene (CTV) units connected by three aliphatic linkers. In the case of cryptophane-E (Chart 1), the linkers are propylene residues. This molecule can act as a host accommodating a small guest inside its cavity. It has been found^{17,18} that, among a variety of small neutral molecules (mostly halogenated hydrocarbons), the most

[†] Stockholm University.

[‡] University of Central Oklahoma.

[§] Present address: Laboratory of NMR Spectroscopy, Institute of Chemical Technology, CZ-166 28 Prague 6, Czech Republic.

(1) (a) Gutsche, C. D. *Calixarenes*; The Royal Society of Chemistry: Cambridge, 1989. (b) Gutsche, C. D. *Calixarenes Revisited*; *ibid.*, 1998.

(2) Diederich, F. *Cyclophanes (Monographs in Supramolecular Chemistry)*; The Royal Society of Chemistry: Cambridge, 1991.

(3) *Crown Ethers and Cryptands*; Gokel, G. W., Ed.; The Royal Society of Chemistry: Cambridge, 1989.

(4) Schneider, H.-J.; Hackett, F.; Rüdiger, V. *Chem. Rev.* **1998**, *98*, 1755–1785.

(5) Schramm, U.; Roesky, C. E. O.; Winter, S.; Rechenbach, T.; Boeker, P.; Lammers, P. S.; Weber, E.; Bargon, J. *Sens. Actuators, B* **1999**, *57*, 233–237.

(6) Bergeron, R. J.; Burton, P. S. *J. Am. Chem. Soc.* **1982**, *104*, 3664–3670.

(7) Bergeron, R. J.; Channing, M. A. *J. Am. Chem. Soc.* **1979**, *101*, 2511–2516.

(8) Higler, I.; Timmerman, P.; Verboom, W.; Reinhoudt, D. N. *Eur. J. Org. Chem.* **1998**, 2689–2702.

(9) Cram, D. J.; Tanner, M. E.; Keipert, S. J.; Knobler, C. B. *J. Am. Chem. Soc.* **1991**, *113*, 8909–8916.

(10) Potter, M. J.; Kirchhoff, P. D.; Carlson, H. A.; McCammon, J. A. *J. Comput. Chem.* **1999**, *20*, 956–970.

(11) Kobayashi, K.; Asakawa, Y.; Kikuchi, Y.; Toi, H.; Aoyama, Y. *J. Am. Chem. Soc.* **1993**, *115*, 2648–2654.

(12) Bartik, K.; Luhmer, M.; Dutasta, J. P.; Collet, A.; Reisse, J. *J. Am. Chem. Soc.* **1998**, *120*, 784–791.

(13) Brotin, T.; Lesage, A.; Emsley, L.; Collet, A. *J. Am. Chem. Soc.* **2000**, *122*, 1169–1174.

(14) Luhmer, M.; Goodson, B. M.; Song, Y. Q.; Laws, D. D.; Kaiser, L.; Cyrier, M. C.; Pines, A. *J. Am. Chem. Soc.* **1999**, *121*, 3502–3512.

(15) Garell, L.; Dutasta, J. P.; Collet, A. *Angew. Chem., Int. Ed. Engl.* **1993**, *32*, 1169–1171.

(16) Canceill, J.; Lacombe, L.; Collet, A. *C. R. Acad. Sci., Ser. 2* **1987**, *304*, 815–818.

(17) Canceill, J.; Lacombe, L.; Collet, A. *J. Am. Chem. Soc.* **1986**, *108*, 4230–4232.

(18) Canceill, J.; Cesario, M.; Collet, A.; Guilhem, J.; Lacombe, L.; Lozach, B.; Pascard, C. *Angew. Chem., Int. Ed. Engl.* **1989**, *28*, 1246–1248.

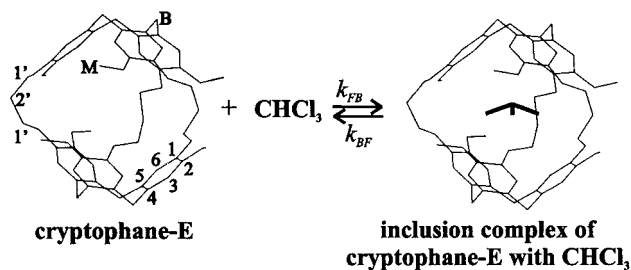


Figure 1. Scheme of the inclusion complex formation and definition of the reaction rate constants. The complex structure is taken from an X-ray crystal structure,¹⁸ hydrogen atoms are not displayed.

stable complex of cryptophane-E is formed with chloroform (see Figure 1).

The crystal structure of the complex¹⁸ reveals that the chlorine atoms of chloroform are situated in the equatorial plane of the cryptophane, while the hydrogen is pointing toward the CTV unit (right-hand side of Figure 1). Concerning the polar orientation of the chloroform guest, a disorder in the crystal structure was encountered, suggesting that the guest can adopt two positions in the cavity, providing an effective D_3 symmetry. The question of rotational mobility of the guest in this inclusion complex has been addressed only by computational methods thus far.¹⁹ We wish to address this issue from the experimental point of view.

Figure 1 also shows the definition of reaction-rate constants k_{FB} , k_{BF} . The effective chemical exchange rates k^*_{FB} , k^*_{BF} required for interpretation of NMR experiments are given as: $k^*_{FB} = k_{FB}[\text{cryptophane-E}]$, $k^*_{BF} = k_{BF}$ (square brackets denote molar concentration). The association constant K_1 is defined according to eq 1.

$$K_1 = \frac{[\text{cryptophane-E-CHCl}_3]}{[\text{cryptophane-E}][\text{CHCl}_3]} \quad (1)$$

NMR relaxation measurements represent a well-established tool to quantify rotational molecular dynamics.²⁰ They have been used to shed light on a great variety of problems in systems ranging from small solvent molecules to synthetic and biological macromolecules. For the description of motion of large and middle-sized molecules, the Lipari–Szabo “model-free” approach²¹ has been proven to be very useful. It was derived from just a few basic assumptions concerning the molecular motion (vide infra), and it uses a rather limited set of parameters that can be calculated often from a quite limited set of NMR relaxation measurements.

The characterization of the motion of a small guest molecule is more difficult because, commonly, even less experimental data are available for a potentially more complicated motion inside the host’s cavity. To quantify the degree of coherence of molecular motion of the guest and the host in an inclusion complex, the concept of motional coupling, expressed as a ratio of the rotational correlation times of the guest and of the host, has been introduced.^{6,7,22–24} The utilization of this concept relies

on the selection of appropriate motional models for the two species, because the values of correlation times are model-dependent. The most common choice is that of rigid, isotropic rotors.^{6,25–28} This model has obvious shortcomings (it does not allow for internal motion or overall anisotropy) and can be expected to function best in the case of very weakly coupled motions and a rather symmetric guest.

We will show that treating the whole complex as a single molecule within the framework of the Lipari–Szabo approach is a better choice in the case of strong motional coupling. This approach corresponds to a physical picture involving a strongly anisotropic van der Waals interaction that effectively behaves as a normal directional bond, allowing only a certain degree of rotational mobility around the bond axis.

We also stress that an appropriate consideration of chemical exchange, corresponding to the process of complex formation and dissociation, is necessary. Such a consideration is often neglected in the literature,^{23,27} if the exchange appears slow on the ^1H chemical shift scale. The sequence of steps, involving several experiments and the use of appropriately modified Bloch equations for the extraction of the longitudinal relaxation times and the heteronuclear steady-state nuclear Overhauser enhancement (NOE) from the relaxation measurements, is presented for the case of slow chemical exchange.

The Modified Bloch Equations for Relaxation in the Presence of Chemical Exchange. The ^{13}C longitudinal relaxation due to the dipole–dipole interaction with the directly bound protons is single exponential, under the conditions of ^1H decoupling. The spin–lattice relaxation time, T_1 , can be extracted from the standard inversion–recovery experiment (delay – π -pulse – mixing time – $\pi/2$ -pulse – FID) by simple exponential fitting of peak intensities as a function of the mixing time. The nuclear Overhauser enhancement factor ($1 + \eta$) of the ^{13}C signal due to ^1H saturation is conveniently measured by omitting the π -pulse in the sequence above, switching the decoupler on at the beginning of the mixing time, making the measurement with one very short and one very long mixing time, and taking the ratio of the peak intensities in the two spectra (the dynamic NOE sequence).²⁹ However, in the presence of exchange between different chemical states, the extraction of these relaxation parameters, specific for each state, becomes more complicated.

If the exchange occurs on a time scale similar to that of the nuclear relaxation, the modified Bloch equations³⁰ can be used to describe the course of the nuclear spin system toward equilibrium.

$$\frac{d}{dt} \begin{pmatrix} I_F \\ I_B \end{pmatrix} = \begin{pmatrix} -R_F - k^*_{FB} & k^*_{BF} \\ k^*_{FB} & -R_B - k^*_{BF} \end{pmatrix} \begin{pmatrix} I_F \\ I_B \end{pmatrix} + \begin{pmatrix} R_F & 0 \\ 0 & R_B \end{pmatrix} \begin{pmatrix} (1 + \eta_F)I_F^0 \\ (1 + \eta_B)I_B^0 \end{pmatrix} \quad (2)$$

(19) Varnek, A.; Helissen, S.; Wipff, G.; Collet, A. *J. Comput. Chem.* **1998**, *19*, 820–832.

(20) Levy, G. C.; Kerwood, D. J. *Encyclopedia of Nuclear Magnetic Resonance*; Grant, D. M., Harris, R. K., Eds. Wiley: New York, 1996; pp 1147–1157.

(21) Lipari, G.; Szabo, A. *J. Am. Chem. Soc.* **1982**, *104*, 4546–4559.

(22) Behr, J. P.; Lehn, J.-M. *J. Am. Chem. Soc.* **1976**, *98*, 1743–1747.

(23) Hilmersson, G.; Rebek, J., Jr. *Magn. Reson. Chem.* **1998**, *36*, 663–669.

(24) Brevard, C. H.; Kintzinger, J. P.; Lehn, J.-M. *Tetrahedron* **1972**, *28*, 2447.

(25) Inoue, Y.; Okuda, T.; Miyata, Y. *Carbohydr. Res.* **1982**, *101*, 187–195.

(26) Inoue, Y.; Kuan, F.-H.; Chujo, R. *Bull. Chem. Soc. Jpn.* **1987**, *60*, 2539–2545.

(27) Mock, W. L.; Shih, N.-Y. *J. Am. Chem. Soc.* **1989**, *111*, 2697–2699.

(28) Azaroual-Belanger, N.; Perly, B. *Magn. Reson. Chem.* **1994**, *32*, 8–11.

(29) Kowalewski, J.; Ericsson, A.; Vestin, R. *J. Magn. Reson.* **1978**, *31*, 165.

(30) Ernst, R.; Bodenhausen, G.; Wokaun, A. *Principles of Nuclear Magnetic Resonance in One and Two Dimensions*; Oxford University Press: Oxford, 1994.

The set of equations (eq 2) describes longitudinal relaxation of the spin states I_F , I_B that correspond to the ^{13}C nucleus of CHCl_3 in the free (index F) or the bound (index B) states. R_F , R_B are the longitudinal relaxation rates ($R_F = 1/T_{1F}$, $R_B = 1/T_{1B}$).

Here, we should point out the different equilibrium- or steady-states that can occur in the system and, consequently, in the equations. When the spin system is allowed to relax in the absence of any radio frequency irradiation, the equilibrium magnetizations I_F^0 , I_B^0 are proportional to the macroscopic concentrations of the free and host-bound forms. If the longitudinal relaxation takes place under the condition of ^1H saturation (without any chemical exchange present), the equilibrium magnetization at $t \rightarrow \infty$ is NOE-enhanced by the factors of $(1 + \eta_F)$, $(1 + \eta_B)$, respectively. When, in addition, the chemical exchange is present, the magnetizations at $t \rightarrow \infty$ are denoted as I_F^∞ , I_B^∞ and can be obtained as a limit of the modified Bloch equations (eq 2). The NOEs for the two states (NOE_F, NOE_B) can be thus determined using the classical dynamic NOE pulse sequence and eq 3.

$$\text{NOE}_F = (1 + \eta_F) = \frac{k_{FB}^* I_F^\infty - k_{BF}^* I_B^\infty}{R_F I_F^0} + \frac{I_F^\infty}{I_F^0}$$

$$\text{NOE}_B = (1 + \eta_B) = \frac{k_{BF}^* I_B^\infty - k_{FB}^* I_F^\infty}{R_B I_B^0} + \frac{I_B^\infty}{I_B^0} \quad (3)$$

The last term of eq 3 represents the standard formula for determination of the steady-state NOE by taking the ratio of signals from spectra with very long and zero mixing times. The first term corresponds to the effect of chemical exchange.

The overall strategy that we adopt for deriving the relaxation rates in the free and bound states of chloroform is as follows. First, the exchange rates are determined from the proton 1D NOESY (EXSY) experiment. In the second step, ^{13}C longitudinal relaxation rates R_F , R_B are determined from an inverse detected inversion–recovery experiment (see the Experimental Section) by fitting the dependence of the signal intensities of the bound and free forms on the mixing time to the numerical solution of the set of equations (eq 2) (employing the previously measured effective exchange rates). In the third step, the NOE parameters for the free and bound chloroform carbons are obtained from an inverse detected dynamic NOE experiment.

Basic Equations of the Lipari–Szabo Approach. The most efficient nuclear relaxation mechanism under the experimental conditions of this study is the dipole–dipole (DD) interaction between directly bonded ^{13}C and ^1H nuclei. In addition, the chemical shielding anisotropy (CSA) mechanism is also effective for aromatic nuclei; therefore, their relaxation is not analyzed in this paper. The DD–CSA cross-correlation contribution to the longitudinal relaxation is removed by ^1H decoupling during the relaxation period.

Neglecting the nondipolar mechanisms and cross-correlation between DD interactions, the longitudinal relaxation time T_1 , and NOE factor $(1 + \eta)$ can be expressed in terms of spectral densities at linear combinations of ^1H and ^{13}C resonance frequencies.³¹ The proportionality factor (the square of the dipole–dipole coupling constant, DCC) depends on the sixth power of the CH distance r_{CH} as well as several universal constants (permeability of vacuum μ_0 , ^{13}C and ^1H magnetogyric ratios γ_C , γ_H , and Planck constant h). N_H denotes the number of attached hydrogens.

$$T_1^{-1} = \frac{1}{4} N_H (\text{DCC})^2 [J(\omega_H - \omega_C) + 3J(\omega_C) + 6J(\omega_H + \omega_C)] \quad (4)$$

$$\eta = \left(\frac{\gamma_H}{\gamma_C} \right) \frac{6J(\omega_H + \omega_C) - J(\omega_H - \omega_C)}{J(\omega_H - \omega_C) + 3J(\omega_C) + 6J(\omega_H + \omega_C)} \quad (5)$$

$$\text{DCC} = \left(\frac{\mu_0 \gamma_C \gamma_H h}{8\pi^2} \right) r_{\text{CH}}^{-3} \quad (6)$$

To express the frequency dependence of the spectral densities (and thus of the relaxation parameters) one needs to adopt a certain model for the molecular motion. Lipari and Szabo²¹ derived the spectral densities under the assumptions that the molecule rotates isotropically as a whole (with the global correlation time τ_M) and that individual CH vectors, in addition, undergo a much faster (and uncorrelated with the global rotation) local motion of a limited amplitude. The local motion is described by two parameters: a generalized order parameter S^2 (defining the degree of restriction) and the local correlation time τ_e .

$$J(\omega) = \frac{2}{5} \left[\frac{S^2 \tau_M}{1 + \omega^2 \tau_M^2} + \frac{(1 - S^2) \tau_e}{1 + \omega^2 \tau_e^2} \right] \quad (7)$$

$$\tau^{-1} = \tau_M^{-1} + \tau_e^{-1}$$

The simple model of a rigid body isotropic rotation can be viewed as a limiting case of the Lipari–Szabo model with totally restricted local motions, $S^2 = 1$.

$$J(\omega) = \frac{2}{5} \left[\frac{\tau_M}{1 + \omega^2 \tau_M^2} \right] \quad (8)$$

The ^{13}C relaxation becomes magnetic field dependent if $\omega\tau > \sim 1$ at the relevant angular frequencies, which provides an opportunity to sample the spectral densities at several frequencies.

Experimental Section

The sample used in this study consisted of cryptophane-E (purchased from Acros Chemicals) in the concentration of $0.01 \text{ mol} \cdot \text{dm}^{-3}$, of chloroform in the concentration of $0.037 \text{ mol} \cdot \text{dm}^{-3}$ (Aldrich Chemical Co.), and of tetrachloroethane- d_2 (Cambridge Isotope Laboratories) as solvent. In addition, methylene chloride was found in the sample in the concentration of $0.005 \text{ mol} \cdot \text{dm}^{-3}$. It most probably filled the cavity in the raw cryptophane-E as obtained from the supplier. All of the compounds were used as obtained without further purification or stabilization. The sample was degassed using the freeze–pump–thaw procedure (three times) and flame-sealed in a 10 mm NMR tube.

The spectra were acquired on a Bruker AC 250 (5.9 T) spectrometer at room temperature and on Varian Inova spectrometers (9.4 and 14.1 T) at 303 K using the standard temperature-control units. All of the quantitative experiments were repeated at least twice, and the average values are reported. The ^1H and ^{13}C signals were assigned using the standard COSY and INEPT experiments at 9.4 T.

The chemical exchange between chloroform free and bound sites was measured at 14.1 T using a ^1H 1D NOESY³² sequence employing a half-Gaussian pulse. The bound state was excited with 20 ms, and the free state with 10 ms selective $\pi/2$ -pulses (the hard ^1H $\pi/2$ -pulse duration was 32 μs). Thirteen values of mixing time were used, ranging between 0 and 0.35 s or between 0 and 1.2 s when exciting the bound and the free state, respectively. The effective rates were determined as linear terms of a second-order polynomial fitted to the build-up curve.

(31) Abragam, A. *The Principles of Nuclear Magnetism*; Clarendon Press: Oxford, 1961.

(32) Kessler, H.; Anders, U.; Gemmecker, G.; Steuernagel, S. *J. Magn. Reson.* **1989**, *85*, 1–14.

The signal intensities were normalized to the integrated intensity of the excited signal at zero mixing time (obtained by extrapolation of the second-order polynomial, which best fits the mixing time dependence of the excited signal integral intensity). The recycle time was 68 s (more than 5 times the apparent T_1 of the free chloroform ^1H resonance).

The ^{13}C longitudinal relaxation times and $^{13}\text{C}\{-^1\text{H}\}$ steady-state NOEs of cryptophane-E nuclei were measured in all three magnetic fields using the fast inversion recovery (FIR)³³ and dynamic NOE²⁹ sequences, respectively. The spectral window typically covered 140 ppm, the spectrum size was 32 K, and the numbers of transients were 3200–4000, 3600, 500–1500, and $\pi/2$ -pulse durations were 10, 9, 10.5 μs , at 5.9, 9.4, 14.1 T, respectively. The Waltz-16 scheme was used for decoupling with the power adjusted to give the decoupling $\pi/2$ -pulse duration $> 90 \mu\text{s}$. At least eight values of variable delay were used in FIR; the recycle delay was always longer than 3 times the longest measured T_1 . The T_1 values were determined from peak intensities by three-parameter exponential fitting. For NOE measurements, one very short and one long ($> 8 \times T_1$) proton irradiation delay was used. The recycle delay was 8–10 times the longest T_1 . The NOE factor ($1 + \eta$) was determined as the ratio of peak intensities in the two spectra.

The host-bound and free chloroform ^{13}C relaxation times were measured at 14.1 T in an inverse manner using the INEPT-enhanced inversion–recovery sequence.³⁴ The reason for the choice of the inverse detection scheme is the fact that the ^{13}C signal of the bound CHCl_3 is hidden under the strong solvent signal. The method works in a differential manner, that is two subsequent scans differ by the orientation of the z -magnetization at the beginning of the relaxation period, and the resulting FIDs are subtracted. The initial conditions of the relaxation for the first scan are (n stands for signal enhancement due to starting INEPT segment):

$$\begin{aligned} I_{\text{F}}(0) &= -nI_{\text{F}}^0 \\ I_{\text{B}}(0) &= -nI_{\text{B}}^0 \end{aligned} \quad (9)$$

Similarly, the initial conditions for the spin states for the second scan are:

$$\begin{aligned} I_{\text{F}}(0) &= nI_{\text{F}}^0 \\ I_{\text{B}}(0) &= nI_{\text{B}}^0 \end{aligned} \quad (10)$$

The ^{13}C longitudinal relaxation rates for both the free and the bound chloroform states were determined simultaneously by an iterative procedure. In each step, the set of coupled differential equations (eq 2) is solved numerically with the two different initial conditions given by eq 9 and eq 10. The two solutions are then subtracted to provide the mixing time-dependent theoretical signal intensities that are compared with their experimental counterparts, and the deviations are least-squares minimized throughout the iteration. The calculation was performed on a PC using Matlab 5.3.

The $\pi/2$ -pulse duration was 32 μs for ^1H and 11 μs for ^{13}C . The delays for magnetization transfer and refocusing were set to match a J_{CH} of 210 Hz. The carrier frequency was set to the middle between the ^1H resonances of free and bound chloroform species. No ^{13}C decoupling during acquisition was applied so as not to include the artifact central band intensity (due to incomplete suppression of the signal of the ^{12}C -bound protons) to the measured sidebands. The Waltz-16 scheme was used for ^1H decoupling during the relaxation period at the power level corresponding to a ^1H $\pi/2$ -pulse of 220 μs . The spectrum of 32 K data points covered the window of ca. 10 ppm. Eleven values of variable delay ranging from 0 to 20 s were used.

The $^{13}\text{C}\{-^1\text{H}\}$ steady-state NOE for the chloroform signals was measured in a similar way, taking advantage of the ^1H detection.³⁴ The

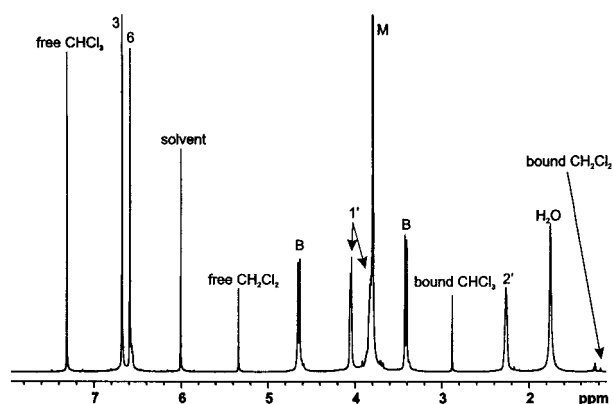


Figure 2. ^1H NMR spectrum of cryptophane-E with CHCl_3 (600 MHz, 303 K) with assignment. Protons are numbered according to the carbon they are attached to.

starting INEPT segment was omitted to obtain the true equilibrium magnetizations I_{F}^0 , I_{B}^0 in the spectrum with zero mixing time. The differential step was omitted as well, to obtain nonzero magnetization at the mixing time $t \rightarrow \infty$. The steady-state NOE was determined from the two spectra—without and with a 30 s initial ^1H irradiation period. The number of transients was 512, and the recycle delay was 48 s. The steady-state NOEs of the two states were evaluated according to eq 3.

Results and Discussion

Kinetics of the Complex Formation. The composition of the mixture was determined by integration of the ^1H NMR spectrum at 600 MHz, compare Figure 2. Because the complexation causes only minor shifts of the cryptophane-E resonances, their integration provides the total amount of the host. Inclusion of chloroform to the host's cavity, however, causes an upfield shift of the guest resonance of 4.44 ppm (the free species resonates at 7.30 ppm, the host-bound one at 2.86 ppm) due to the shielding effect of the cyclotrimerarylene units. The two sites are in mutual slow exchange on the carbon-13 and proton chemical shift time scales. The situation is similar for CH_2Cl_2 , although its lower total concentration and lower association constant give rise to only a trace signal of the complexed species at the position reported by Canceill et al. (1.19 ppm).¹⁸

Thus, the sample consists of $0.0077 \text{ mol}\cdot\text{dm}^{-3}$ cryptophane-E– CHCl_3 complex, $0.0004 \text{ mol}\cdot\text{dm}^{-3}$ cryptophane-E– CH_2Cl_2 complex, $0.0295 \text{ mol}\cdot\text{dm}^{-3}$ free CHCl_3 , $0.0045 \text{ mol}\cdot\text{dm}^{-3}$ free CH_2Cl_2 . The amount of free cryptophane-E, obtained by subtraction of the concentrations of the complexes from the total, is $0.0019 \text{ mol}\cdot\text{dm}^{-3}$. While the concentration ratio of bound to free chloroform (0.26) is determined reasonably accurately from the integrated spectrum, the absolute value of the residual concentration of the free cryptophane is subject to significant uncertainty. The equilibrium constants at 303 K, based on the concentrations above, are $137 \text{ mol}^{-1}\cdot\text{dm}^3$ and $50 \text{ mol}^{-1}\cdot\text{dm}^3$ for CHCl_3 and CH_2Cl_2 , respectively. Because of the uncertainty of the free cryptophane concentration, the equilibrium constant for the chloroform complex can be subject to a large error, perhaps as high as 50%. For the dichloromethane complex the uncertainty is even larger, because of the low concentrations of the free and bound CH_2Cl_2 . It should be stressed that the value of the equilibrium constant is not of real interest for the present study. Canceill and co-workers^{17,18} have studied the complexation equilibria in the same systems and reported substantially higher values of the equilibrium constants ($470 \text{ mol}^{-1}\cdot\text{dm}^3$ for chloroform and about $110 \text{ mol}^{-1}\cdot\text{dm}^3$ for dichloromethane).

(33) Canet, D.; Levy, G. C.; Peat, I. R. *J. Magn. Reson.* **1975**, *18*, 199–204.

(34) Allard, P.; Jarvet, J.; Ehrenberg, A.; Gräslund, A. *J. Biomol. NMR* **1995**, *5*, 133–146.

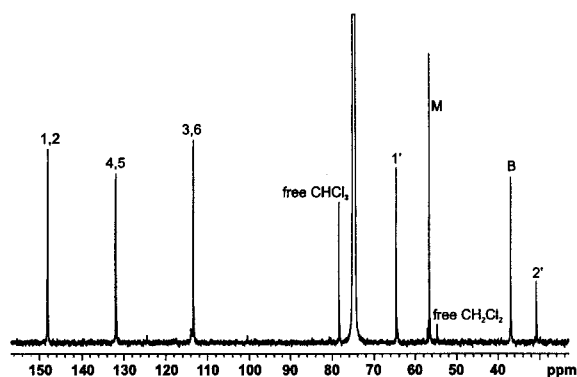


Figure 3. ^{13}C NMR spectrum of cryptophane-E with CHCl_3 (600 MHz, 303 K) with assignment. The weak signals or the broadening of the foot of the host resonances arise from the free cryptophane-E.

Those measurements have been carried out in a way similar to ours, and it appears to us that they also are subject to similar uncertainties. Thus, the two sets of data are not necessarily in conflict with each other.

To measure the relaxation of the guest, it was necessary to establish first the effective exchange rates k_{FB}^* , k_{BF}^* of the chloroform entering and leaving the host molecule. Thanks to the favorable separation of the two exchanging signals, a 1D NOESY was the method of choice. In two separate 1D NOESY experiments, we excited selectively the resonance of either the free or of the bound chloroform. The initial build-up (dependent on mixing time) of the transferred magnetization depends only on a single effective exchange rate, k_{FB}^* or k_{BF}^* , respectively. The effective exchange rates were determined rather precisely: $k_{\text{FB}}^* = 0.168 \text{ s}^{-1}$ ($\pm 0.010 \text{ s}^{-1}$), $k_{\text{BF}}^* = 0.621 \text{ s}^{-1}$ ($\pm 0.020 \text{ s}^{-1}$). The error estimates are based on comparisons of different ways to evaluate the initial rates. The ratio $k_{\text{FB}}^*/k_{\text{BF}}^* = 0.27$ is in excellent agreement with the ratio of signal integrals of the two forms in the ^1H spectrum (0.26), which provides an independent check of accuracy. Our rate constants are also lower than the corresponding values of Canceill et al.^{17,18} To our understanding, their results were obtained using the proton linewidth/lineshape measurements at variable temperature. At the particular temperature of our experiments, where the exchange leads to very small line broadening, we believe that our 1D NOESY measurements give more accurate rates.

The 1D NOESY experiment did not reveal any NOE contacts of the bound chloroform proton with any of the protons of cryptophane-E. The distances of the chloroform proton from the protons of the CTV unit estimated from the crystal structure¹⁸ are 410–440 pm, and that is probably too far to observe an NOE using a sample prepared for optimal ^{13}C sensitivity, and in the presence of chemical exchange. In addition, we did not observe any splitting of the host resonances due to an asymmetric position of the guest inside the cavity. This is probably because the inclusion of chloroform to the cavity has only a very small effect on the host chemical shifts (as opposed to the large effect of the CTV units of the host on the chloroform resonances).

NMR Relaxation of the Host. The ^{13}C spectrum of cryptophane-E, shown in Figure 3, contains 10 lines. While the signals from the aromatic carbons give rise to three nearly degenerate pseudodoublets, the other carbons provide well-separated singlets. Considering the composition of the sample and the large association constant, we measure predominantly the relaxation of the chloroform-complexed host, with only a slight contribution from the other forms that can well be neglected. It is reasonable to assume that the motion of the host

Table 1. Measured ^{13}C Longitudinal Relaxation Times T_1 and Steady State ^{13}C - $\{^1\text{H}\}$ NOE ($1 + \eta$) for Cryptophane-E Host and Chloroform

carbon	n protons	5.7 T		9.4 T		14.1 T	
		T_1 (ms)	($1 + \eta$)	T_1 (ms)	($1 + \eta$)	T_1 (ms)	($1 + \eta$)
3,6	1	137	2.02	182	1.74	214	1.46
B	2	83	2.05	123	1.93	148	1.55
1'	2	89	2.05	126	1.88	165	1.59
2'	2	85		114	1.81	157	1.59
M	3	414	2.40	523	2.26	589	2.20
bound CHCl_3	1					350	1.52
free CHCl_3	1					11900	3

Table 2. Local Motional Parameters Obtained from Lipari–Szabo Analysis of Relaxation Data of the Inclusion Complex of Cryptophane-E with CHCl_3 ^a

carbon	S^2	$\Delta S^2(\%)$	τ_e (ps)	$\Delta\tau_e(\%)$
B	0.79	6	56	55
1'	0.69	8	44	55
2'	0.70	7	59	42
M	0.065	12	15	13
bound CHCl_3	0.68	11	22	69

^a ΔS^2 , $\Delta\tau_e$ are relative standard deviations of the parameter sets obtained from Monte Carlo simulation.

complexed with CH_2Cl_2 will not be considerably different and that the very small amount of this complex can hardly affect the results. The contribution of the free cryptophane-E species to the evaluated intensities is further reduced by a tiny chemical shift difference (cf. Figure 3) from the resonances of interest.

The ^{13}C longitudinal relaxation times, T_1 , and the NOEs of all secondary and tertiary carbons were measured and are summarized in Table 1. Significantly shorter $N_{\text{H}}T_1$ values (T_1 's after multiplication by the number of attached protons N_{H}) and smaller NOEs for the aromatic nuclei provide an indication of a chemical shield anisotropy (CSA) contribution to the nuclear relaxation, which is difficult to quantify. Consequently, only the dipolar interaction dominated relaxation of the bridging methylene carbons C-B; of the aliphatic linker carbons C-1', C-2' and of the methoxy groups C-M was used for the determination of the rotational dynamics of the host. For all of these carbon resonances, we note that the T_1 and NOE values are field-dependent and that the NOE values are less than the maximum value of 2.99. Thus, we are clearly outside of the extreme narrowing regime.

Cryptophane-E is a fairly spherically shaped molecule, according to the crystal structure data,¹⁸ and the Lipari–Szabo model²¹ can be expected to be suitable for obtaining the relation between the nuclear relaxation and the molecular motions. We fitted simultaneously all of the measured relaxation parameters for the four ^{13}C nuclei to the model (eq 7) to determine nine parameters: S^2 and τ_e for all four carbons and one global correlation time τ_M , common for the whole molecule. The CH distance, determining the dipolar coupling constant (eq 6) was set to 109.8 pm, as in our earlier relaxation studies^{35,36} ($\text{DCC} = 1.434 \times 10^5 \text{ rad}\cdot\text{s}^{-1}$).

We obtained a good fit with the global correlation time of 0.67 ns and the order parameter S^2 of 0.7–0.8 for the different methylene carbons (all of the fitted parameters are shown in Table 2). The order parameters show that the whole molecule is rather rigid, with the propylene linkers slightly more mobile than the methylene bridges between the aromatic rings. The local

(35) di Bari, L.; Mäler, L.; Kowalewski, J. *Mol. Phys.* **1995**, *84*, 31–40.

(36) Mäler, L.; Lang, J.; Widmalm, G.; Kowalewski, J. *Magn. Reson. Chem.* **1995**, *33*, 541–548.

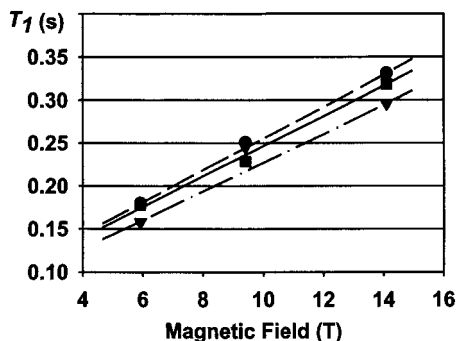


Figure 4. Experimental values of ^{13}C relaxation time T_1 of cryptophane-E methylene residues, and their calculated magnetic field dependence (eq 4): C-1' (●, dashed line), C-2' (■, solid line), C-B (▼, dash-dotted line).

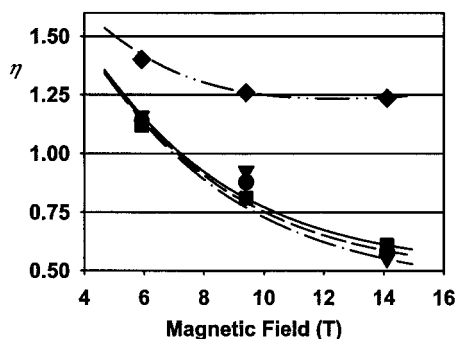


Figure 5. Experimental values of $^{13}\text{C}\{-^1\text{H}\}$ steady-state NOE (η) of cryptophane-E methylene and methyl residues, and their calculated magnetic field dependence (eq 5): C-1' (●, dashed line), C-2' (■, solid line), C-B (▼, dash-dotted line), C-M (◆, dash-dot-dotted line).

correlation times, τ_e , for the three types of methylene groups turned out to be about 50 ps (an order of magnitude faster than the global reorientation), with large uncertainties (see Table 2). In the case of highly restricted local motion (large order parameter S^2), it is only possible to obtain an estimate of the correlation times of the local motion. On the other hand, the fast local correlation time is significantly better determined for the methyl group, which is characterized by a very low-order parameter, indicating almost free rotation. The errors were estimated using a Monte Carlo simulation assuming 5% error in T_1 and 10% in η values. The relative standard deviations found are 8% for S^2 and τ_M , and 50% for τ_e . The quality of the fit is further illustrated in Figures 4 and 5, displaying the magnetic field dependence of the relaxation times and of the heteronuclear NOE factors, respectively.

NMR Relaxation of the Guest. The ^{13}C signal of the bound CHCl_3 is hidden under the strong solvent signal at 75 ppm (the complexation-induced shift is about 3.5 ppm). Since the proton signals of bound and free chloroform are well separated and easy to quantify, it was possible to measure chloroform relaxation using ^1H detection. Because of the chemical exchange between the two sites taking place on the time scale similar to that of nuclear relaxation, it was necessary to use a more elaborate approach (described above) to extract relaxation times and cross-relaxation constants from the signal intensities. The dependencies of the free and the bound chloroform signal intensities on the mixing time (in the INEPT enhanced inversion recovery experiment) and the fitted curves are shown in Figure 6.

The bound-guest relaxation turned out to be rather hard to measure due to low concentration ($0.0077 \text{ mol}\cdot\text{dm}^{-3}$). In addition, in the case of chemical exchange-coupled relaxation,

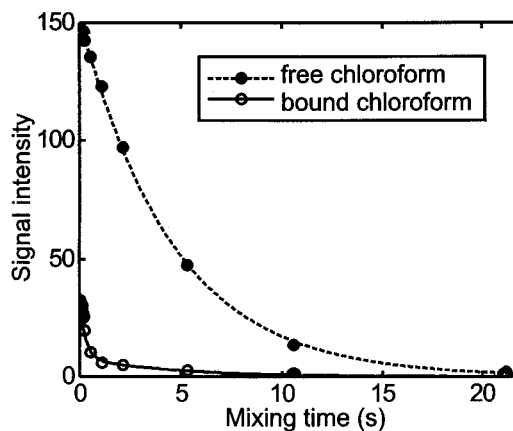


Figure 6. Multiexponential, chemical exchange-coupled ^{13}C longitudinal relaxation of CHCl_3 in the free and in the bound positions. The experimental intensities and the fitted curves (eq 2) are to an arbitrary scale.

the slow decay of the nuclear magnetization of the free guest ($T_1 = 12 \text{ s}$) contributes to the need of long delays in the sequence (mixing time, recycle delay). Thus, only measurements at 14.1 T gave a sufficient signal-to-noise level. The determined relaxation parameters for chloroform are included in Table 1.

Different models can be chosen to interpret the relaxation parameters of the bound chloroform in terms of motional parameters. One choice concerns the carbon-proton distance and the dipolar coupling constant (DCC). We chose here a common value of 109.8 pm for all of the CH bonds in the complex, that is, including chloroform. The CH distances in similar compounds vary between 107 and 112 pm,^{37,38} depending on the system and the experimental methodology used for their determination. Moreover, it is also possible that interaction with the host could influence the CH bond length in chloroform. Because it is necessary to treat the motion of the two species in a consistent manner to be able to make comparisons, we decided to use the same distance of 109.8 pm for both species.

The isotropic reorientation model (eq 8) provides the simplest description of the reorientational dynamics. Using this model, we could obtain a global correlation time for the bound chloroform of about 0.5 ns, which is rather close to Lipari-Szabo τ_M for the host, indicating a strong dynamic coupling. However, the quality of the fit is rather low, and the result depends strongly on the weighting of the two experimental parameters (T_{1B} , η_B). The similarity of the correlation times of the guest and of the host leads us to another model: treating the bound chloroform as an integral part of the host molecule in the framework of the Lipari-Szabo approach (eq 7). In this case, the global correlation time must be common, equal to the one determined for the host (0.67 ns). The order parameter and the local correlation time can be now calculated for the guest from the T_1 and NOE data at a single field (see Table 1). The motional parameters and their errors are listed in Table 2. The uncertainties were estimated by Monte Carlo simulation assuming 10% error bounds in the experimental values. The order parameter for the guest agrees well with the corresponding values for the propylene linkers, which suggests that treating the complex as a single molecule within the Lipari-Szabo approach is correct. Clearly, we should note the strong correlation of the order parameter, the global correlation time, and

(37) *Tables of Interatomic Distances and Configuration in Molecules and Ions*; Chemical Society: London, 1958.

(38) *Tables of Interatomic Distances and Configuration in Molecules and Ions*; Chemical Society: London, 1965.

dipolar coupling constant that contains a value for the CH bond length that is subject to uncertainties. However, independently of these quantitative uncertainties, we can conclude that the order parameter would be substantially lower in the case of a nearly isotropic rotation (or jumps) in the cavity. Thus, this study shows that the van der Waals interaction, even in a rather symmetric system, can be highly anisotropic, behaving as a strong directional bond. Two additional comments should be made about the motion of chloroform inside the cryptophane-E cavity. First, it should be pointed out that this study deals with motion of CH vectors and thus cannot contribute to the question of chloroform rotation about the CH bond axis. Second, the measurements that we have performed are sensitive to fast motions. Thus, we cannot exclude the possibility that the chloroform executes jumps within the cavity on a time scale slower than the reorientation of the complex. This notion should be kept in mind when comparing our findings to the X-ray data.¹⁸

Our results are in conflict with molecular dynamics simulations of the complexation of cryptophane-E by Varnek *et al.*¹⁹ After having adjusted some of the interaction potential parameters to reproduce the relative affinities of the host with respect to different guests, they arrived at a characteristic time of jumps between different chloroform orientations inside the cavity of 20–60 ps, depending on the parameters used. Our interpretation of the discrepancy is that there may be a need for further work on the intermolecular potentials in systems with strong and anisotropic nonbonding interactions.

Our choice to use the Lipari–Szabo model for both the guest and the host makes the concept of motional coupling, involving a comparison of the global correlation times of the interacting species, less useful. In fact, in the situation where the isotropic guest rotation model provides strong motional coupling, we

believe that it is generally more useful to consider the whole complex rather than the two species separately.

Conclusions

The results of this study show that a combined, ¹H and ¹³C NMR exchange and relaxation study has great potential for the investigation of guest–host complexes. The ¹H exchange spectroscopy is a well-established tool for this type of work. Here, we went further with the analysis of the dynamic processes on a much shorter time scale by using ¹³C relaxation.

The analysis of the inversion–recovery and NOE experiments had to be done with caution in the presence of chemical exchange occurring on the same time scale as that of spin relaxation. If this is done, it becomes possible to probe spectral densities at different frequencies by performing experiments at several magnetic fields. Reorientational dynamics of the whole inclusion complex can be then described in terms of the Lipari–Szabo model.

With regard to the complex-bound guest, we find that chloroform behaves as an integral part of the host cryptophane-E molecule after inclusion in its cavity. No fast large scale motion of chloroform inside the cavity was observed. The cryptophane-E–chloroform complex thus represents a van der Waals molecule with a long lifetime (on the time scale of molecular reorientation) and with strongly anisotropic (directional) interaction between the cyclotrimeratrylene unit of the host and the hydrogen of the guest.

Acknowledgment. This research was supported by the Swedish Natural Science Research Council. J.J.D. acknowledges support by the Office of Sponsored Research and Grants of the University of Central Oklahoma.

JA004349Y